Development 133, 2539-2551 (2006) doi:10.1242/dev.02427

Dachs: an unconventional myosin that functions downstream of Fat to regulate growth, affinity and gene expression in *Drosophila*

Yaopan Mao[1,*], Cordelia Rauskolb[2,*], Eunjoo Cho[1,†], Wei-Li Hu[3,‡], Heather Hayter[3], Ginny Minihan[3], Flora N. Katz[3,§] and Kenneth D. Irvine[1,¶]

The *dachs* gene was first identified almost a century ago based on its requirements for appendage growth, but has been relatively little studied. Here, we describe the phenotypes of strong *dachs* mutations, report the cloning of the *dachs* gene, characterize the localization of Dachs protein, and investigate the relationship between Dachs and the Fat pathway. Mutation of *dachs* reduces, but does not abolish, the growth of legs and wings. *dachs* encodes an unconventional myosin that preferentially localizes to the membrane of imaginal disc cells. *dachs* mutations suppress the effects of *fat* mutations on gene expression, cell affinity and growth in imaginal discs. Dachs protein localization is influenced by Fat, Four-jointed and Dachsous, consistent with its genetic placement downstream of *fat*. However, *dachs* mutations have only mild tissue polarity phenotypes, and only partially suppress the tissue polarity defects of *fat* mutants. Our results implicate Dachs as a crucial downstream component of a Fat signaling pathway that influences growth, affinity and gene expression during development.

KEY WORDS: *Dachs*, Myosin, Leg, Wing, *fat*, Growth, Protocadherin, *Drosophila*

INTRODUCTION

Adult structures of the head, thorax and genitalia in *Drosophila* develop from clusters of undifferentiated cells in the larva called imaginal discs. The discs grow throughout the three larval instars, and then evert and differentiate during pupal development to form the adult cuticle. The growth and patterning of imaginal discs is governed by highly conserved intercellular signaling pathways (reviewed by Irvine and Rauskolb, 2001; Klein, 2001; Lawrence and Struhl, 1996), including Notch, Wnt, Egf, Hedgehog and Bmp pathways. Imaginal discs have proven to be an outstanding model for identifying and characterizing components of these pathways. Recent work has led to the suggestion that disc growth and patterning are also dependent upon a new signaling pathway, the Fat pathway.

fat encodes a large protocadherin (Mahoney et al., 1991). Genetic studies in *Drosophila* have identified three crucial requirements for *fat* during imaginal disc development. First, *fat* is required to limit wing growth, as mutation of *fat* causes disc overgrowth (Bryant et al., 1988). Second, *fat* acts cell-autonomously to influence an intercellular signaling process between distal and proximal wing cells that establishes a ring of Wingless (Wg) expression in the proximal wing (Cho and Irvine, 2004). Third, *fat* plays a crucial role in the establishment of tissue polarity (Casal et al., 2002; Rawls et al., 2002; Strutt and Strutt, 2002; Yang et al., 2002).

[1]Howard Hughes Medical Institute, Waksman Institute and Department of Molecular Biology and Biochemistry, Rutgers The State University of New Jersey, Piscataway, NJ 08854, USA. [2]Waksman Institute, Rutgers The State University of New Jersey, Piscataway, NJ 08854, USA. [3]Department of Biology, Texas A&M University, College Station, TX 77843-3258, USA.

*These authors contributed equally to this work
[†]Present address: RIKEN Center for Developmental Biology, 2-2-3 Minatojima-minamimachi, Chuo-ku, Kobe, 650-0047, Japan
[‡]Present address: PO Box 371, 29 Palms, CA 92277, USA
[§]Present address: Fogarty International Center, N.I.H., 31 Center Drive MSC 2220, Bethesda, MD 20892-2220, USA
[¶]Author for correspondence (e-mail: irvine@waksman.rutgers.edu)

Accepted 4 May 2006

The molecular basis for the influence of *fat* on these processes has not been determined, but genetic studies have identified genes that function together with *fat* (Adler et al., 1998; Casal et al., 2002; Cho and Irvine, 2004; Rawls et al., 2002; Strutt and Strutt, 2002; Yang et al., 2002). Two, *four-jointed* (*fj*) and *dachsous* (*ds*), act genetically upstream of *fat* in the regulation of tissue polarity (Yang et al., 2002), and act non-autonomously to influence the expression of Wg in the proximal wing (Cho and Irvine, 2004). *ds* encodes a protocadherin (Clark et al., 1995) that appears to participate in heterophilic interactions with Fat (Ma et al., 2003; Matakatsu and Blair, 2004; Strutt and Strutt, 2002). These observations suggest that Ds and Fat might bind each other to mediate intercellular signaling, with Ds acting as a ligand and Fat as a receptor. *fj* encodes a protein found in both secreted (Villano and Katz, 1995) and Golgi-resident (Strutt et al., 2004) forms, and might influence Fat-Dachsous interactions.

A third gene that has been genetically linked to *fat* is *dachs*, which was first described by Bridges and Morgan (Bridges and Morgan, 1919). The original *dachs* mutant allele, d^1, results in reduction of wing and leg growth similar to that observed in alleles of *fj* and *ds* (Waddington, 1940; Waddington, 1943). *dachs* also interacts genetically with *fj* to influence leg segmentation and growth (Buckles et al., 2001), suggesting that its function is related to these Fat pathway components. More recently, *dachs* was shown to be epistatic to *fat* both for the regulation of *wg* expression in the proximal wing, and for imaginal disc growth (Cho and Irvine, 2004). These observations suggest that *dachs* might act as a downstream component of Fat signaling. However, the nature and extent of the requirement for *dachs* has not been well understood because only one allele was characterized, and the molecular nature of Dachs had not been described.

Here, we present the first phenotypic characterization of strong mutations in *dachs*. These mutations define requirements for *dachs* in different *fat*-dependent processes. We also show that *dachs* encodes an unconventional myosin, and characterize its subcellular localization. Finally, we show that the localization or stability of

Dachs at the membrane is influenced by Fat signaling, thus providing molecular evidence that Dachs is a downstream component of a Fat signaling pathway.

MATERIALS AND METHODS

Drosophila genetics

The d^{210}, d^{GC2} and d^{GC13} alleles were the kind gift of F. Michael Hoffmann. For male recombination (Chen et al., 1998), a stock was constructed to contain two flanking markers for the area of interest, *black* (*b*) and *clot* (*cl*), as well as a source of P transposase (Robertson et al., 1988). *w; cl*^{1} *d*^{1} *b*^{1}*/Cyo*; *Sb*Δ*2-3/TM6B* flies were crossed to a set of P element insertion stocks (Fig. 5A). Recombination in males is confined to these P insertion sites. For each P-element, 22-28 crosses were set up and 1500-3000 progeny were screened. *dachs* phenotypes were analyzed using the d^{1}, d^{210}, d^{GC2} and d^{GC13} alleles, in homozygous, transheterozygous, and hemizygous combinations, using *Df(2L)N22-5* and *Df(2L)ED623*. We also examined d^{GC13} *ck*^{13}, *fat*^{8}, *fat*$^{G\text{-}rv}$, d^{GC13} *fat*^{8}, d^{1} *fat*^{8}, d^{GC13} *fat*$^{G\text{-}rv}$, *ft*^{d1}, *ds*^{UA071}, and *ds*^{36D} mutant animals.

UAS-d insertions were isolated on the second (*UAS-d[2D]*, *UAS-d[2A]*) and third (*UAS-d[2B]*) chromosomes. *UAS-d:V5* insertions were isolated on the second (*UAS-d:V5[50-5]*, *UAS-d:V5[18-4]*) and third (*UAS-d:V5[9-F]*, *UAS-d:V5[18-2]*, *UAS-d:V5[8-3]*) chromosomes. Rescue and overexpression experiments were conducted by crossing to *tub-Gal4*, *arm-Gal4*, *C765Gal4*, *ptc-Gal4* or *da-Gal4*. Ectopic expression clones were created by Flp-out using the *UAS-d* and *UAS-d:V5* lines, as well as the following stocks: *y w hs-Flp[122]*; *act>y*$^{+}$*>Gal-4 UAS-GFP (AyGal4)*; *UAS-fj*; *GS-ds*; *UAS-fat*; *UAS-fat*; *UAS-d:V5[9F]*; *UAS-fj*; *UAS-d:V5[9F]*; and *GS-ds*; *UAS-d:V5[9F]*.

Simple mutant clones were created using FLP-FRT mediated recombination, with the following stocks: *y w;* d^{GC13} *FRT40A/CyO-GFP*; *y w;* d^{1} *FRT40A/CyO-GFP*; *y w;* fat^{8} *FRT40A/CyO-GFP*; *y w;* $fat^{G\text{-}rv}$ *FRT40A/L14*; *y w;* d^{GC13} fat^{8} *FRT40A/CyO-GFP*; d^{GC13} *ck*^{13} *FRT40A/CyO-GFP*; *y w;* d^{1} fat^{8} *FRT40A/CyO-GFP*; *y w hs-flp[122]; Ubi-GFP FRT40A*; *w hs-flp[122] f; M(2)25A P[f*$^{+}$*30B] FRT40A*; *y w hs-flp[122];* y^{+} *FRT40A/CyO*; *y w hs-flp[122]; M(2)25A Ubi-GFP FRT40A/CyO*.

To examine Dachs:V5 expression in fat mutant clones we used *y w;* $ft^{G\text{-}rv}$ *FRT40A; UAS-d:V5[9F]/L14* × *y w hs-FLP; Ubi-GFP FRT40A; C765Gal4* and related stocks, substituting *UAS-d:V5[18-2]*, *tub-Gal4* or *arm-Gal4*.

Molecular biology

For RFLP analysis of *dachs* mutant DNA, probes were prepared by XL PCR (Perkin-Elmer) based on sequence in GadFly across the 70 kb interval indicated in Fig. 5. Candidate genes were then amplified by PCR from wild-type and mutant DNA.

The identification of *dachs* was communicated to GenBank by F.K. prior to publication (Accession Number AF405293). FlyBase (Drysdale and Crosby, 2005) currently lists three transcripts for *dachs*, d-RA, d-RB and d-RC. d-RA (Accession Number NM_175991) differs slightly from the original submission of AF405293, but is consistent with BDGP EST sequences and our own more recent sequence analysis of cDNAs and RT-PCR products, and encodes the product depicted in Fig. 5; the entry for AF405293 has thus been corrected to match d-RA. d-RB and d-RC correspond to *Myo29D* transcripts reported by Tzolovsky et al. (Tzolovsky et al., 2002), but we were unable to detect them by RT-PCR from larval total RNA. *dachs* cDNAs were recovered from a third instar cDNA library enriched for imaginal discs (Brown and Kafatos, 1988). We also prepared cDNA by RT-PCR from total RNA using either Superscript II reverse transcription (GibcoBRL) or OneStep RT-PCR kit (Qiagen). For construction of *UAS-dachs*, cDNA fragments were prepared by RT-PCR and then cloned into pGEM-T (Promega) to make a cDNA corresponding to nucleotides 52-3915 of d-RA, which was then verified by DNA sequencing. Plasmid pUAST-d was constructed by cloning nucleotides 71-3915 of *dachs* into pUAST using *Eco*RI and *Not*I; the start codon begins at nucleotide 71. A CCACC Kozak sequence was introduced in front of the ATG. V5-tagged Dachs was created by replacing the stop codon and 3′ UTR of *dachs* with V5 and His_6 sequences from pMTBip/V5-His (Invitrogen).

Histology, Immunohistochemistry and western blotting

Imaginal discs were fixed and stained as described previously (Cho and Irvine, 2004), using as primary antibodies rabbit anti-V5 (1:1000, Novus), mouse anti-V5 (1:200, Invitrogen), rat anti-Fat intracellular domain (1:100. H. McNeill), mouse anti-Wg (1:800, 4D4, DSHB), rat anti-Ser (1:1000) (Papayannopoulos et al., 1998), goat anti-β-gal (1:1000, Biogenesis), rat anti-Elav (1:40, 7E8A10, DSHB), mouse anti-Dac (1:40, DSHB), rat anti-DE-Cad (1:40, DSHB), mouse anti-Dll (1:400) (Duncan et al., 1998) and mouse anti-Prospero (1:50, DSHB).

In situ hybridization was carried out as described previously (Rauskolb and Irvine, 1999), using a labeled antisense RNA probe corresponding to nucleotides 1710-3915 of the predicted *dachs* transcript.

Western blotting was performed on larval tissue (wing, leg and haltere discs, attached to fragments of cuticle) boiled in SDS-PAGE loading buffer. The Dachs:V5 was detected with mouse anti-V5 (Invitrogen).

Examination of adult tissues

Mutant clones in adult flies were generated and analyzed as described by Hao et al. (Hao et al., 2003), except that flies were heat-shocked 0-72 hours AEL. Pupal legs were dissected in PBS, fixed for 45 minutes in PLP (McClean and Nakane, 1974), and mounted in fluorescent mounting medium. Polarity was scored in male abdominal segments 2-4. Mutant clones were marked with *yellow*, which is only scorable in bristles; thus, we did not distinguish between autonomous and non-autonomous effects in these experiments. We scored only clones that included more than one bristle; the severity of the polarity phenotype did not correlate with clone size among clones analyzed (2-11 bristles).

RESULTS

dachs alleles

The original *dachs* allele, d^{1}, is viable, with shortened legs and wings (Bridges and Morgan, 1919; Waddington, 1940; Waddington, 1943). The reduction in wing length is most obvious in the middle of the wing, as evidenced by the reduced distance between the cross veins (Fig. 1B, compare with 1A). As each cell in the wing normally secretes a single hair, the number and spacing between hairs serves as a measure of cell number and size. Counting hairs between the crossveins in d^{1} mutants revealed that the reduction in inter-crossvein distance is associated with a corresponding decrease in cell number (not shown).

To better define requirements for *dachs*, additional alleles were characterized. The strength of these alleles was then evaluated by examining the phenotypes of homozygous, hemizygous and transheterozygous animals. This analysis identified two alleles, d^{210} and d^{GC13}, that are stronger than d^{1}, and another allele, d^{GC2}, that is weak like d^{1} (Figs 1, 2; data not shown). Animals homozygous for d^{210} die by early larval stages, but this likely results from other mutations on the d^{210} chromosome, as d^{GC13} homozygotes survive until the end of pupal development, yet d^{210} behaves similarly to d^{GC13} in combinations with d^{GC13} and d^{1} (Figs 1, 2; data not shown), and molecular analysis (see below) predicts that d^{GC13} encodes a more severely truncated protein than d^{210}. d^{GC13} animals make adult tissue, but usually fail to eclose from the pupal case (less than 1% of animals eclose), forming pharate adults that can be dissected out and examined. The d^{GC13} phenotype is similar in homozygotes and in transheterozygous combinations with *dachs* deficiencies (Figs 1, 2; data not shown), suggesting that it could be a null mutation.

dachs adult phenotypes

The legs of d^{GC13} mutants are more severely affected than d^{1} mutants (Fig. 2). All of the intermediate and distal segments of the leg (femur through tarsus) are noticeably shortened, and some tarsal segments are fused, typically resulting in the formation of only three tarsal segments instead of the normal five. Although each of the genes in

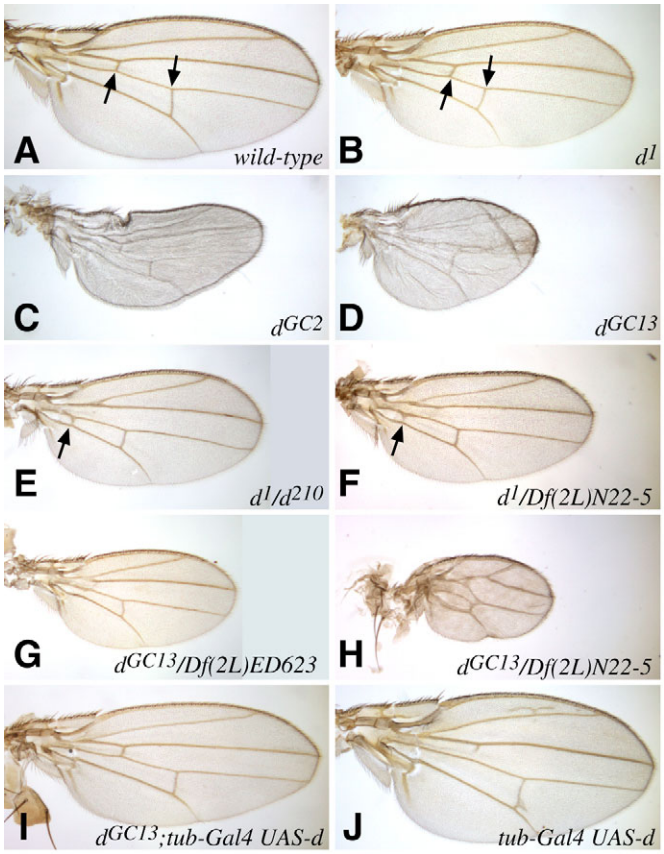

Fig. 1. Requirements for *dachs* in the wing. Adult wings, all at the same magnification, from (**A**) wild type, (**B**) d^1, (**C**) d^{GC2}, (**D**) d^{GC13}, (**E**) d^1/d^{210}, (**F**) $d^1/Df(2L)N22-5$ and (**G**) $d^{GC13}/Df(2L)ED623$. This wing came from exceptional individual that eclosed, and represents the mildest *dachs*-null phenotype observed. (**H**) $d^{GC13}/Df(2L)N22-5$. (**I**) d^{GC13}; *tub-Gal4 UAS-d:V5[18-2]* (**J**) *tub-Gal4 UAS-d:V5[8-3].* Arrows in A,B indicate crossveins; arrows in E,F indicate ectopic crossvein material, whereas the anterior crossvein is missing. Wings in C,D,H are from pharate adults.

the Fat pathway influence leg development, their phenotypes are different, presumably reflecting their distinct roles within the pathway (see Fig. S1 in the supplementary material). In addition to a general reduction in length, in some cases no external leg tissue is evident in d^{GC13} mutants, or the leg appears to form a single mass of tissue. Pupal legs, however, are consistently shortened but never absent or severely deformed. Examination of pupae suggested that the legs absent phenotype actually derives from defects in the morphological changes that occur during leg disc eversion (Fig. 2L; data not shown). Indeed, direct examination of d^{GC13} pharate adults revealed that when external legs are absent, masses of leg tissue could be found differentiating within the body cavity (Fig. 2M). The disc eversion phenotype was also observed in d^{GC2}, but not in d^1. To further define the *dachs* leg phenotype, we also characterized d^{GC13} mutants clones. These caused reduced growth and fusions of tarsal segments similar to those observed in mutant animals, but even large mutant clones were not associated with a failure of disc eversion (not shown).

d^{GC13} wings are smaller than d^1 or wild-type wings (Fig. 1). They also exhibit abnormal wing patterning, as evidenced by a variable phenotype that includes extra, missing and mis-positioned crossveins (Fig. 1). Extra or missing crossveins are also often observed in adult flies with d^{GC13} mutant clones, and in d^1/d^{GC13}, d^1/d^{210}, or d^1/Df animals (Fig. 1; data not shown).

Transcriptional targets of *dachs* and *fat*

In wing imaginal discs, clones of cells mutant for *fat* are associated with upregulation of Wg expression in the proximal wing (Cho and Irvine, 2004). Conversely, clones of cells mutant for d^1 exhibit a severe loss of Wg expression in the proximal wing, but this loss of Wg is transient (Cho and Irvine, 2004). To investigate whether the transience of Wg loss in d^1 results from remaining *dachs* activity, we examined d^{GC13} mutant clones, but their affect on Wg expression was similar – Wg is severely reduced at early third instar, but essentially normal by late third instar (not shown).

Clones of cells mutant for *fat* have been reported to be associated with upregulation of *fj* expression in eye imaginal discs (Yang et al., 2002), and we have observed that *fat* mutant clones are also associated with induction of *fj* expression in leg (not shown) and wing (Fig. 3D) imaginal discs, as assayed by a *fj-lacZ* reporter. Importantly then, clones of cells mutant for d^{GC13} are associated with decreased *fj* expression in eyes and wings (Fig. 3A,C). However, the influence of *dachs* on *fj* expression was detected during early and mid-third instar, but not late third instar.

Loss of leg joints and reduced leg growth is characteristic of mutations in genes in the Notch signaling pathway. To evaluate the potential relationship between *dachs* phenotypes and Notch signaling, we investigated the expression of the Notch ligand Serrate (Ser) in discs containing d^{GC13} mutant clones. During third instar, loss of Ser could not be detected (Fig. 3F). Some loss of Ser expression could be detected in pupal legs in regions where *dachs* mutation is associated with leg segment fusions (Fig. 3I), but it is not clear in this context whether loss of Ser is a cause or a consequence of the loss of leg tissue. Nonetheless, Fj (Buckles et al., 2001) and Ds (data not shown) can induce the expression of Ser and Delta in neighboring cells when ectopically expressed in the leg. These observations suggest that the Fat pathway does have a role in regulating Notch ligand expression during leg development. To further evaluate this, we examined Ser expression in clones of cells mutant for *fat*. *fat* mutant clones could be associated with ectopic Ser expression, although this was preferentially observed in the proximal leg (Fig. 3G). Within the proximal leg (defined for these experiments as proximal to the *dachshund* expression domain), 36/47 *fat* clones exhibited an obvious upregulation of Ser expression. Thus, *fat* has a normal role in repressing Ser expression during leg development. An influence of *fat* on Notch ligand expression probably accounts for the occasional outgrowths of leg tissue observed in *fat* mutants and in association with *fat* mutant clones (Bryant et al., 1988; Mahoney et al., 1991) (Fig. 2I), as these outgrowths appear similar to those observed upon ectopic Notch activation (Rauskolb and Irvine, 1999).

Prior work has identified a set of broadly expressed genes, the leg gap genes, that are responsible for the initiation of Notch ligand expression in the leg (Rauskolb, 2001). To position the action of Fat within the leg segmentation hierarchy, we examined the expression of two key leg gap genes, *dachshund* and *Distal-less*. Both of these genes were expressed normally within *fat* mutant clones (not shown), suggesting that the action of Fat in leg segmentation is downstream of these broadly expressed genes.

Epistasis of *dachs* to *fat*

dachs suppresses the consequences of *fat* mutation on wing disc growth (Cho and Irvine, 2004). Moreover, even though *dachs* mutation does not lead to permanent loss of Wg expression in the

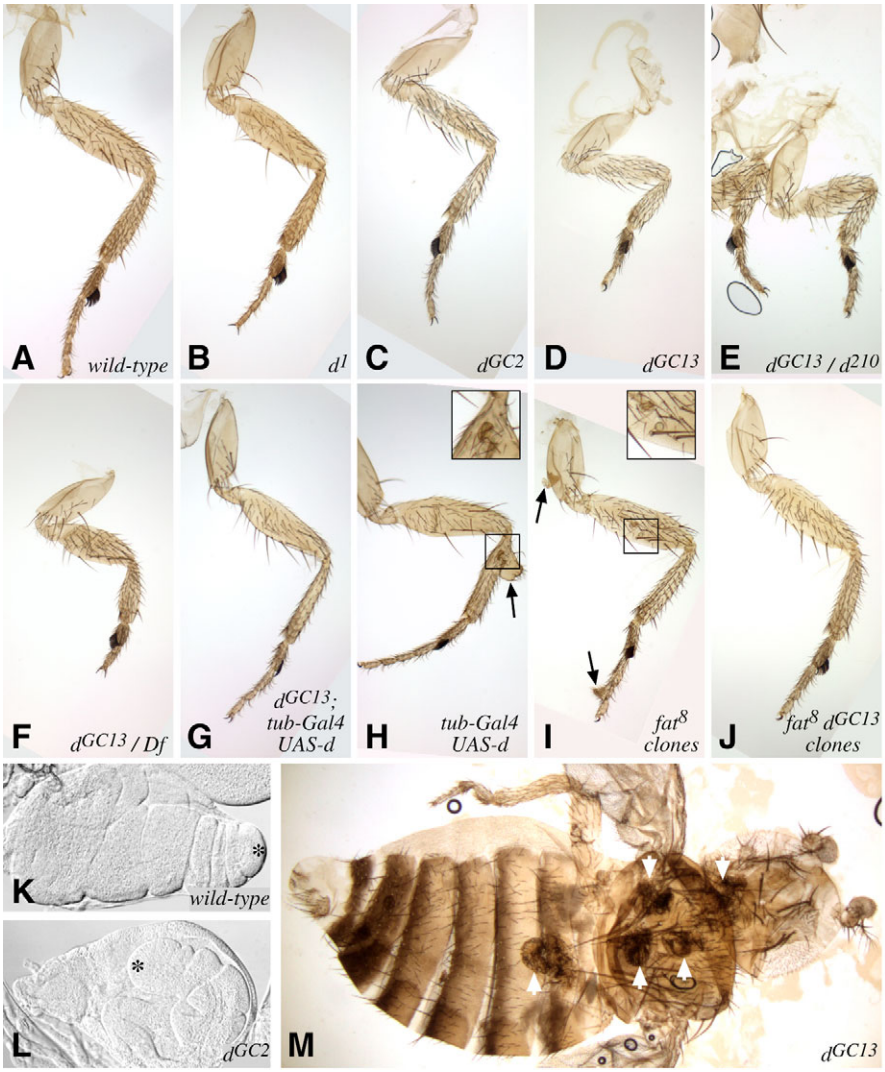

Fig. 2. Requirements for *dachs* in the leg. Panels A-J show adult legs, all at the same magnification, from (**A**) wild type, (**B**) d^1, (**C**) d^{GC2}, (**D**) d^{GC13}, (**E**) d^{GC13}/d^{210}, (**F**) $d^{GC13}/Df(2L)ED623$, (**G**) d^{GC13}; *tub-Gal4 UAS-d:V5[18-2]* , (**H**) *tub-Gal4 UAS-d:V5[8-3]* , (**I**) an animal with fat^8 mutant clones and (**J**) an animal with fat^8 d^{GC13} double mutant clones. In H and I, arrows indicate outgrowths and insets show internal cuticle vesicles. (**K-L**) Pupal legs from wild type and d^{GC2}, the tip of the leg (asterisk) is mispositioned in L. (**M**) d^{GC13} pharate adult, with only one external leg and five that failed to evert (arrowheads).

proximal wing, it nonetheless completely suppresses the ability of *fat* mutation to induce ectopic Wg expression (Cho and Irvine, 2004) (Fig. 4). To further evaluate the hypothesis that *dachs* is a general downstream component of a Fat pathway, we evaluated the ability of *dachs* to suppress additional *fat* mutant phenotypes, and to suppress *fat* phenotypes in other tissues.

Even though mutation of *dachs* has little effect on Ser expression in the legs of otherwise wild-type animals, *dachs* completely suppresses the Ser expression induced by *fat* mutation (Fig. 3H, 0/37 *fat dachs* double mutant clones in the proximal leg exhibited upregulation of Ser). Additionally, mutation of *dachs* suppresses the ability of *fat* mutant clones to induce outgrowths in adult legs (Fig. 2J: 12/50 legs with *fat* mutant clones had outgrowths, but 0/62 legs with *fat dachs* clones had outgrowths). *dachs* also suppresses the induction of *fj* expression associated with mutation of *fat* (Fig. 3E).

Another striking feature of *fat* mutant clones is their roundness (Fig. 4A). Normally, clones of cells adopt irregular, elongated shapes. However, genetic manipulations that influence cell affinity cause clones to be rounder and smoother. Strikingly, mutation of *dachs* also suppresses the roundness of *fat* clones (Fig. 4C, see Table S1 in the supplementary material), suggesting that *dachs* is required for an altered affinity of *fat* mutant clones. A difference in cell affinity probably also accounts for the appearance of internal vesicles of cuticular tissue within the legs of animals containing *fat* mutant clones (Fig. 2I: 40/50 legs with *fat* clones had internal vesicles). The appearance of these vesicles is suppressed by mutation of *dachs* (Fig. 2J: 0/62 legs with *fat dachs* clones had internal vesicles). Examination of clone size also confirmed that the suppression of *fat* mutant overgrowth by *dachs* is observed not only at the level of the whole disc (Cho and Irvine, 2004), but also within individual clones (Fig. 4C, see Table S1 in the supplementary material). Altogether, these results indicate that *dachs* is epistatic to *fat* for multiple phenotypes, including gene expression, growth and cell affinity, and in multiple tissues.

Effects of *dachs* on tissue polarity

Another crucial function of *fat* is to regulate tissue polarity (Casal et al., 2002; Rawls et al., 2002; Strutt and Strutt, 2002; Yang et al., 2002). To investigate the possibility that *dachs* influences polarity, we examined d^{GC13} mutant animals and d^{GC13} mutant clones. Planar polarity is evident throughout most of the adult cuticle in the polarized orientation of hairs and bristles. In *fat* mutants, the normal orientation is disturbed, and swirling patterns of hairs and bristles occur in many tissues (e.g. Fig. 5B). It has been reported that d^1 can have mild polarity phenotypes in the leg (Held et al., 1986). We examined d^{GC13} for polarity phenotypes in wings, legs, abdomens

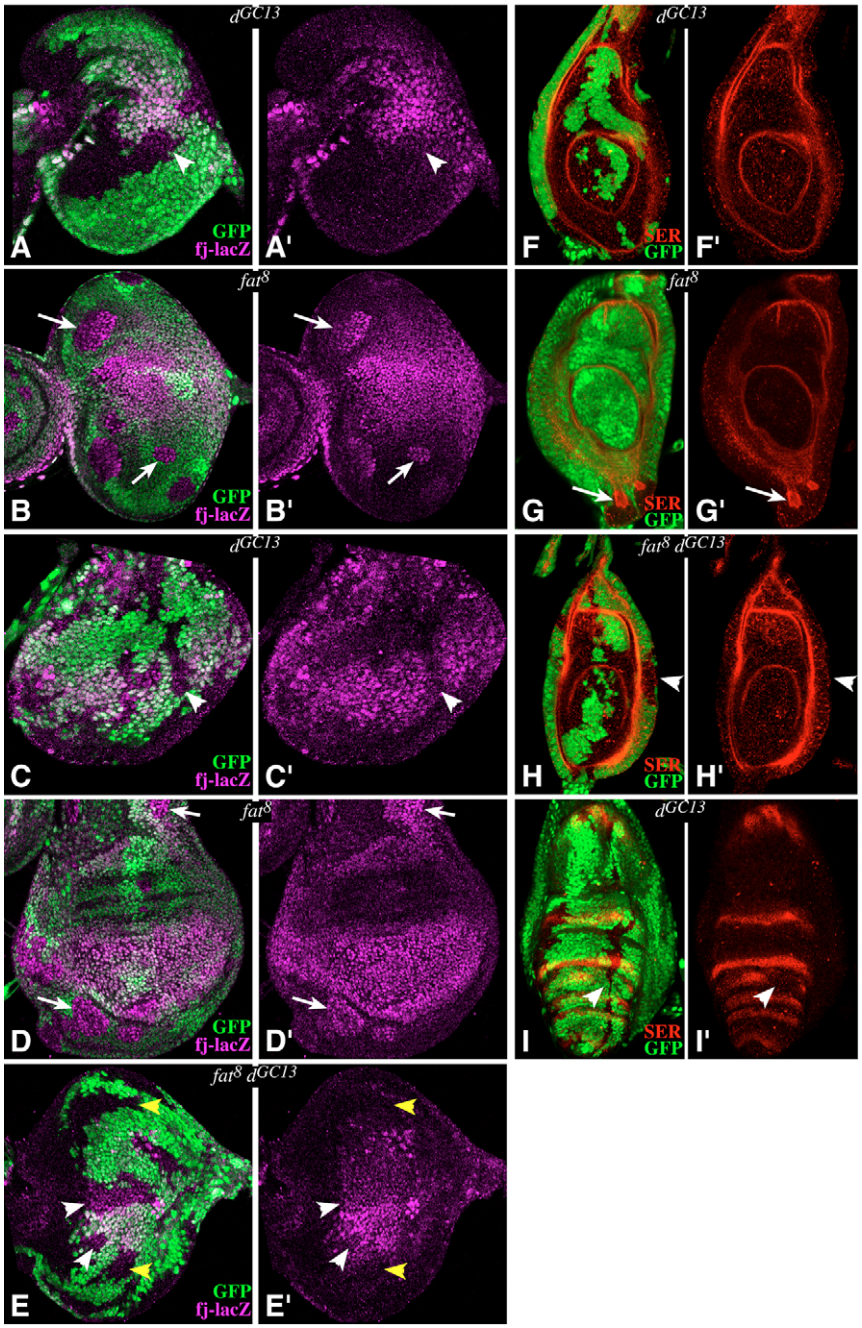

Fig. 3. Influence of *fat* and *dachs* on downstream target genes. Imaginal discs, with wild-type cells marked by GFP (green), stained for Ser (red) or *fj-lacZ* (magenta) expression. In this and subsequent figures, panels marked ′ show individual channels of the panel to the left. Arrows indicate examples of ectopic or elevated expression, arrowheads indicate examples of reduced or absent expression. (**A**) Eye disc with reduced *fj-lacZ* within d^{GC13} mutant clones. (**B**) Eye disc with elevated *fj-lacZ* within fat^{8} clones. (**C**) Wing disc with reduced *fj-lacZ* within d^{GC13} clones. (**D**) Wing disc with elevated *fj-lacZ* within fat^{8} clones. (**E**) Eye disc with reduced *fj-lacZ* within fat^{8} d^{GC13} mutant clones (white arrowheads), and no ectopic *fj-lacZ* (yellow arrowheads). (**F**) Leg disc with normal Ser expression within large (*Minute*) d^{GC13} clones. (**G**) Leg disc with ectopic Ser within proximal fat^{8} clones (**H**) Leg disc with normal Ser expression (arrowhead) within large (*Minute*) proximal fat^{8} d^{GC13} clones. (**I**) Pupal leg disc with reduction of Ser expression within the second tarsal segment.

and eyes. Only mild polarity phenotypes were observed. As in wild-type animals, hairs in the abdomen point posteriorly (Fig. 5D), most leg bristles and wing hairs point distally (Fig. 2, Fig. 5I), and most ommatidia are correctly oriented (Fig. 5K).

The relatively mild polarity phenotypes of *dachs* contrast with the strong polarity phenotypes of *fat*, and thus we investigated double mutant animals to determine whether *dachs* is also required for the influence of *fat* on polarity. For these studies, we focused on eyes and abdomens. In the abdomen, *fat* mutant animals exhibit extensive swirling (Fig. 5B) (Casal et al., 2002), *dachs* mutants have no obvious polarity phenotype (Fig. 5D) and *fat dachs* double mutants exhibit an intermediate phenotype (Fig. 5E), in which there is some irregularity in the orientation of abdominal hairs, but they are less disturbed than in *fat* mutants. To provide a quantitative comparison, we scored disturbances in polarity associated with clones of mutant cells in abdominal segments. All (39/39) *fat* clones had polarity phenotypes (Fig. 5C), whereas only 3% (2/60) of *dachs* clones (Fig. 5G) and 54% (37/68) of *fat dachs* clones (Fig. 5F) exhibited polarity phenotypes. There was also a difference in the severity of the polarity phenotypes, as all of the *fat* clones were associated with some hairs at an angle greater than 90° relative to the normal orientation, whereas 26% (18/68) of *fat dachs* clones and 0% of *dachs* clones were associated with hairs at an angle of 90° or greater. In the remaining *fat dachs* clones (19/68), the degree of change in polarity was less severe (Fig. 5F). Thus, mutation of *dachs* partially suppresses polarity phenotypes associated with mutation of *fat* in the abdomen.

Polarity in the eye is manifest in the specification of chiral forms of ommatidia, which differ in their orientation and placement of photoreceptor cells. Staining with a neural marker (Elav) and an R7

marker (Prospero) illustrates the regular polarized orientation of ommatidia in the eye (Fig. 5J). In d^{GC13}, some disorganization in ommatidial orientation is observed, indicative of a mild polarity phenotype, but overall polarity is again largely normal (Fig. 5K). To examine the relationship of *dachs* to *fat*, we again focused on animals containing clones of mutant cells. *fat* mutant clones are consistently associated with strong polarity phenotypes (Rawls et al., 2002; Strutt and Strutt, 2002; Yang et al., 2002), which include completely reversed ommatidia (Fig. 5M, 32/33 *fat* clones included ommatidia rotated more than 90° away from normal), whereas *dachs* mutant clones exhibited mild polarity phenotypes, with only slightly mis-rotated ommatidia (Fig. 5L, 1/32 *dachs* clones included ommatidia rotated more than 90° away from normal). *fat dachs* double mutant clones appear similar to *fat* (Fig. 5N, 28/33 *fat dachs* clones included ommatidia rotated more than 90° away from normal).

dachs encodes an unconventional myosin

Deficiency mapping and male recombination localized *dachs* to 29D1-2, between the most distal P element used for male recombination mapping (7704) and the distal end of a small non-complementing deficiency [*Df(2L)N22-5*; Fig. 6A]. Correlation with the genomic map (FlyBase, 1999) gave an interval of ~70 kb, containing 14 potential transcripts. We used RFLP analysis throughout this interval to identify a single predicted gene, *CG10595*, which contained an internal deletion in d^{GC2}, and a large insertion in d^{1} (not shown). Subsequent analysis showed that this same candidate gene contained mutations in two other *d* alleles (see below), providing strong evidence that this locus encodes *dachs*.

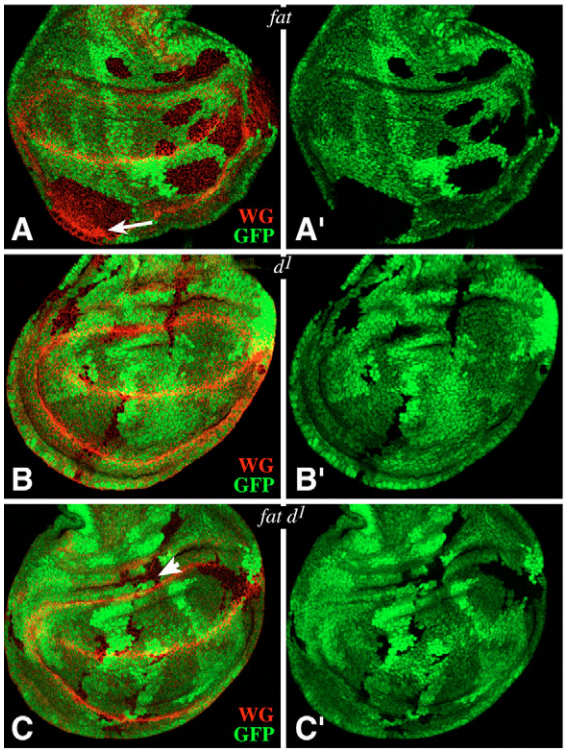

Fig. 4. Influence of *fat* and *dachs* on cell affinity. Third instar wing imaginal discs, stained for expression of Wg (red). GFP (green) marks wild-type cells. (**A**) fat^{8} mutant clones (black) are abnormally large and round. Some elevation of Wg expression in the proximal wing is also visible (arrow), although it is mostly out of the plane focus. (**B**) d^{1} mutant clones have normal, elongated shapes. (**C**) fat^{8} d^{1} double mutant clones lack ectopic Wg expression (arrowhead), and are similar to d^{1} mutant clones in size and shape, and obviously distinct from fat^{8} mutant clones. See also Table S1 in the supplementary material.

Analysis of *dachs* cDNAs and genomic sequences defined seven exons, encoding a predicted protein of 1232 amino acids (Fig. 6). The predicted protein is a member of the Myosin family, identified independently as Myo29D (Tzolovsky et al., 2002). The central region of Dachs includes all of the defining features of a myosin head domain, including a well-conserved ATP binding domain, actin-binding domain and active thiol region (Fig. 6). However, in the middle of the head domain, just before the actin-binding domain, is an unusual insertion of 44 amino acids that is not found in any other Myosin. By blast analysis, the closest mammalian myosins are members of the myosin V, X, and VII families. However, Dachs is not clearly orthologous to any of these mammalian myosins, as the *Drosophila* genome encodes other genes that appear to be more closely related to mammalian myosins V, X, and VII (Tzolovsky et al., 2002).

In addition to the head domain, unconventional myosins sometimes have an N-terminal extension preceding the head domain, which is characteristic for each class (Korn, 2000). Dachs has an N-terminal extension of 235 amino acids that does not have significant similarity to other proteins. As in other myosins, the head domain is followed by neck and tail domains. In Dachs, the neck domain contains a single calmodulin-type IQ-like motif (Fig. 6), the binding site for regulatory light chains. Dachs also encodes a tail domain of 187 amino acids, which does not show extensive similarity to any other proteins. Surprisingly, sequence analysis identifies a potential transmembrane domain C-terminal to the IQ motif, with a predicted type II orientation. This computer prediction has to be treated cautiously, as there is no precedent for transmembrane myosins.

We sequenced the four *dachs* mutant alleles (Fig. 6). d^{GC2} contains a deletion that removes part of the N-terminal extension while retaining the reading frame. d^{1} contains an insertion of the *blood* retrotransposon (Bingham and Chapman, 1986) in the tail domain. *blood* insertions have been reported to affect transcript stability in other genes (Bingham and Chapman, 1986). d^{GC13} and d^{210} are both predicted to encode proteins truncated within the head domain. d^{GC13} contains an 11 bp deletion near the N terminus of the head domain, causing a frame shift followed closely by a stop codon, while d^{210} contains a point mutation that results in a stop codon in the active thiol region (Fig. 6). If the myosin head domain is required for *dachs* function, then both of these mutations would be expected to encode non-functional alleles.

To gain further insight into potential functions of *dachs*, *dachs* expression was examined by in situ hybridization to embryos and imaginal discs. *dachs* mRNA is expressed broadly throughout embryonic and imaginal development, although at certain stages some local upregulation of *dachs* expression was observed (Fig. 7C). Early embryonic expression of *dachs* was near background until stage 9 (Fig. 7), which suggests that there is no significant maternal contribution of *dachs* mRNA.

Based on the identification of Dachs as a myosin, we considered the possibility that *dachs* might be partially redundant with other *Drosophila* myosins. In particular, *crinkled* encodes a *Drosophila* Myosin VII family member (Kiehart et al., 2004), and exhibits a multiple wing hair phenotype, which is also sometimes observed in tissue polarity mutants. To evaluate the possibility of redundancy between *dachs* and *crinkled*, we examined double mutant clones. These displayed both *dachs* and *crinkled* phenotypes, but the

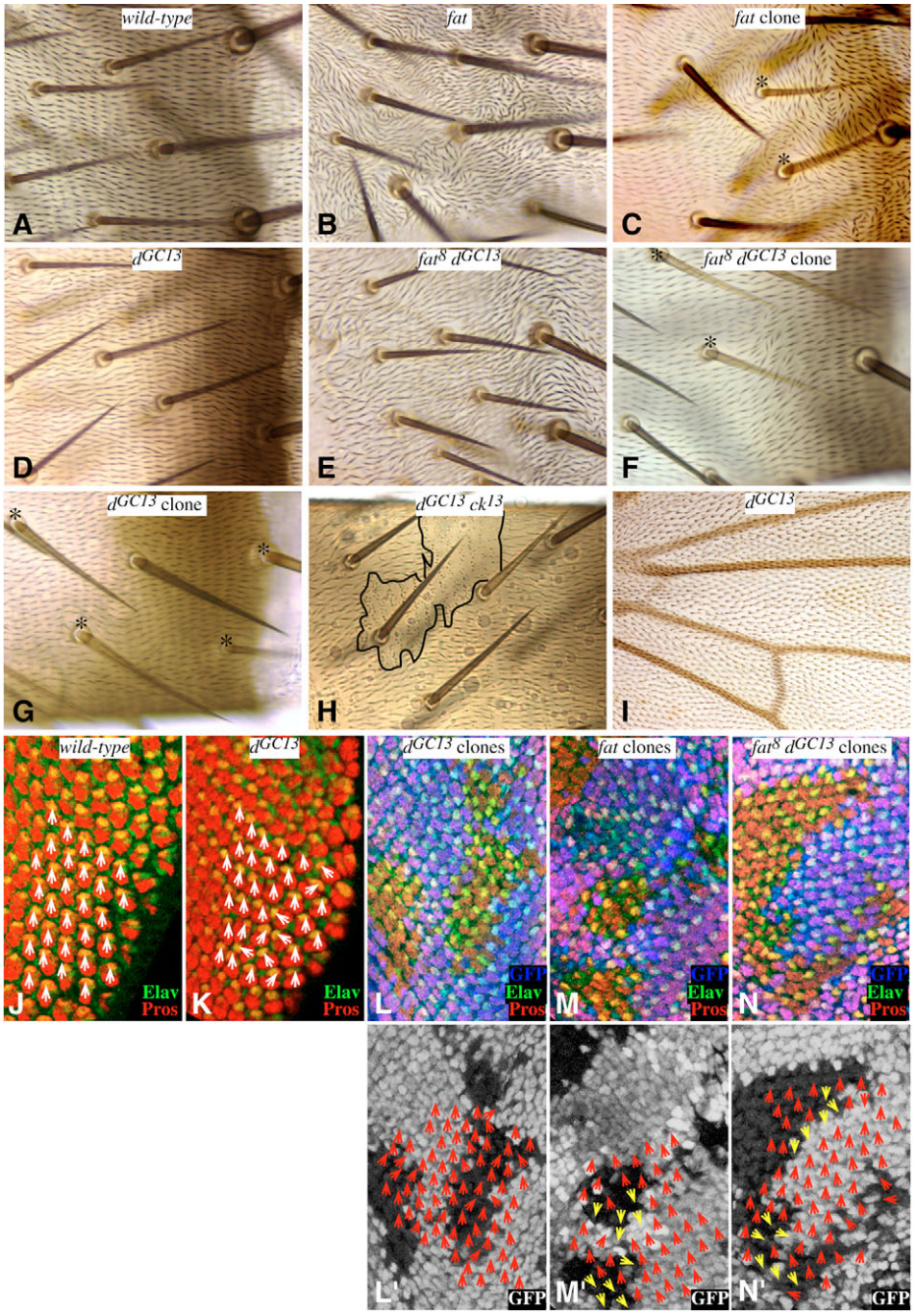

Fig. 5. Influence of *dachs* on polarity. (**A-H**) Regions of abdomens. (C,F,G) Mutant clones, marked by *yellow* bristles (asterisks). (A) Wild type; hairs point posteriorly. (B) $fat^{8}/fat^{G\text{-}rv}$; hair polarity is severely disturbed. (C) fat^{8} mutant clones; hair polarity is severely disturbed. (D) d^{GC13}; hairs point posteriorly. (E) fat^{8} d^{GC13}; hair polarity is moderately disturbed. (F) fat^{8} d^{GC13} mutant clones; hair polarity is moderately disturbed. (G) d^{GC13} mutant clones; hair polarity appears normal. (H) d^{GC13} ck^{13} double mutant clones (outlined); polarity can not be assessed within the clone because of *ck*, but polarity outside the clones appears normal. (**I**) High-magnification of a region of a $d^{GC13}/Df(2L)ED623$ wing, most hairs point distally, as in wild type. (J-N) Eye discs, stained for Elav (red) and Prospero (green). Arrows indicate ommatidial orientation. (**J**) Wild type, (**K**) d^{GC13}. (**L-N**) Mutant clones, marked by absence of GFP (blue in upper panels, white in lower panels). Ommatidia that are mis-rotated by more than 90° are marked by yellow arrows. To compensate for tissue curvature, some panels are composites of multiple focal planes.

phenotypes were not obviously more severe than in the respective single mutants. Thus, loss of Wg expression in the proximal wing was still transient (not shown). Moreover, clones of cells mutant for strong tissue polarity mutants, like *fat*, can influence the polarity of surrounding wild-type cells (Casal et al., 2002), but the polarity of hairs surrounding *dachs crinkled* mutant clones in the abdomen appeared normal (Fig. 5H).

dachs overexpression

Both to confirm the identification of the *dachs* gene, and to evaluate the consequences of Dachs overexpression, we created transgenic animals in which a *dachs* cDNA was expressed under UAS-Gal4 control. When *dachs* is expressed at moderate levels using a *tub-Gal4* driver, apparently normal flies develop. Importantly, expression of *dachs* under *tub-Gal4* control can result in substantial rescue of d^{GC13} mutants, confirming the identification of *dachs*. Both untagged and V5-tagged forms of Dachs were constructed; V5-tagged Dachs can also rescue *dachs* mutations (Fig. 1I, Fig. 2G), indicating that the V5 tag does not significantly impair Dachs function.

High level expression of *dachs*, achieved using different *UAS-dachs* insertions, or by raising animals at higher temperature, can result in disruptions of normal wing and leg development. In the wing, Dachs overexpression increased wing size and resulted in vein abnormalities (Fig. 1J), while in the leg occasional outgrowths of leg tissue and formation of internal vesicles were observed (Fig. 2H). These phenotypes resemble those observed in weak, viable alleles of *fat* (Bryant et al., 1988), consistent with the possibility that

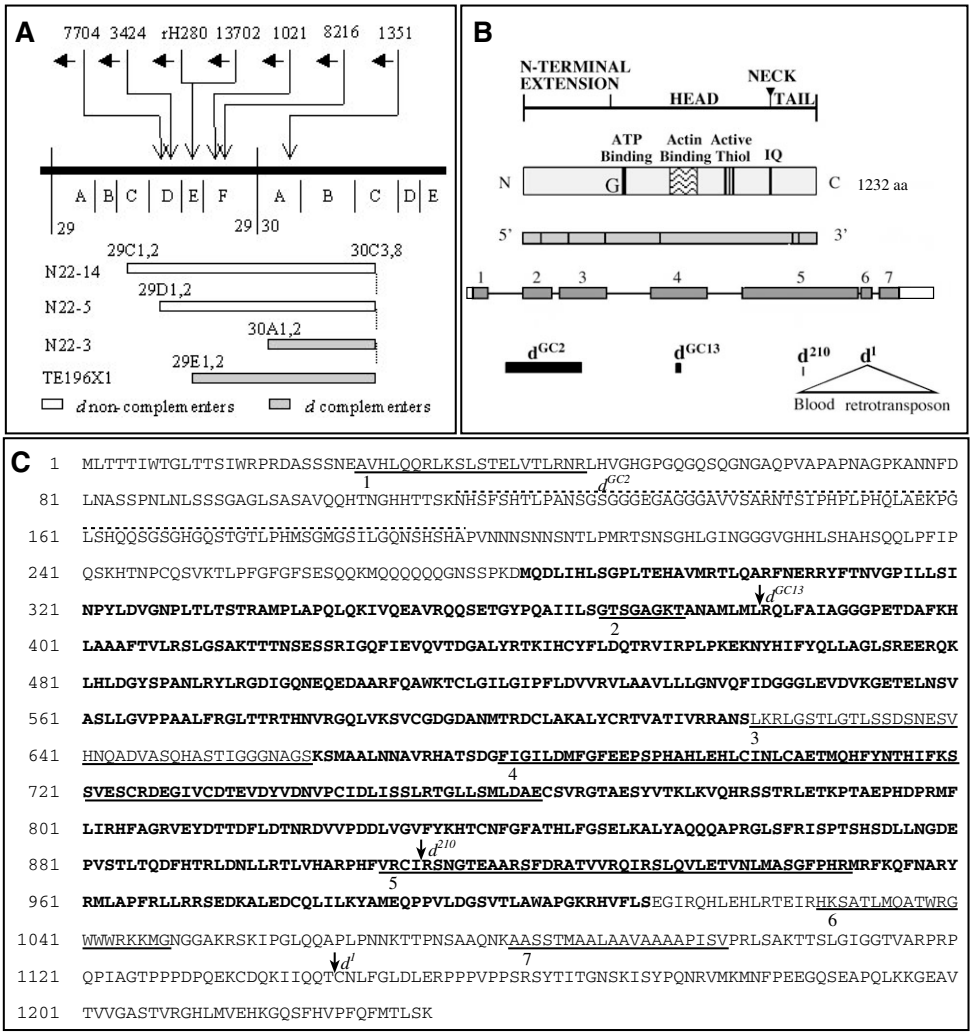

Fig. 6. Cloning and sequence of Dachs. (**A**) Localization of *dachs* on 2L. P elements used for male recombination are indicated above the chromosome. Horizontal arrows indicate the result of recombination, placing *dachs* distal to each insertion. Deficiencies used to map *dachs* are shown below. (**B**) Protein domains, transcript and gene structure of *dachs*. Exons are indicated as boxes and are numbered. Intervening introns appear as black lines. The locations of mutations in *dachs* alleles are indicated. (**C**) Amino acid sequence of Dachs. The conserved myosin head domain is in bold. Underlining identifies motifs discussed in the text: 1, coiled-coil domain; 2, ATP-binding domain; 3, unique insert in myosin head domain; 4, actin-binding domain; 5, active thiol domain; 6, IQ camodulin-binding domain; 7, putative transmembrane domain. The locations of mutations are indicated above: d^{GC2}, inframe deletion indicated by broken line; d^{GC13}, 11 bp deletion predicted to truncate at the indicated aa; d^{210}, point mutation introducing a stop codon; d^{1}, insertion of a blood retrotransposon.

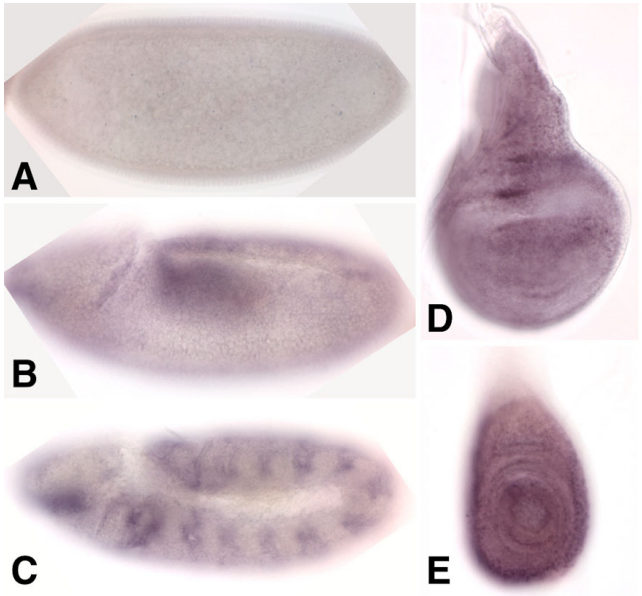

Fig. 7. *dachs* mRNA expression. *dachs* mRNA expression, visualized by in situ hybridization. (**A**) Stage 6 embryo, (**B**) stage 9 embryo, (**C**) stage 11 embryo, (**D**) wing disc and (**E**) leg disc.

downregulation of *dachs* is a crucial *fat* function. Examination of Dachs-expressing clones in adult abdomens did not reveal any effects on polarity (not shown).

As attempts to raise anti-sera against Dachs were unsuccessful, we used V5 epitope-tagged Dachs (Dachs:V5) to characterize the localization of Dachs protein. Immunostaining of *tub-Gal4 UAS-dachs:V5* or *Ay-Gal4 UAS-dachs:V5* animals revealed low-level, diffuse and punctate staining for Dachs in the cytoplasm, and higher levels near the adherens junctions (Fig. 8A,H; data not shown).

Influence of Ds, Fj and Fat on Dachs localization

Genetic studies suggest that Dachs acts as a downstream component of a Fat signaling pathway. However, it was conceivable that Dachs could instead act in parallel to Fat. To further explore the functional connection between Dachs and Fat signaling, we examined Dachs and Fat protein localization under conditions where Fat pathway activity was altered, either by mutation of *fat*, or by overexpression of Fj, Ds or Fat.

Over-expression of either Ds or Fj in clones of cells can result in elevated Fat protein staining at the edge of the clone, with the strongest effects observed where the endogenous expression levels are low (i.e. where there is the greatest contrast between endogenous and ectopic expression) (Cho and Irvine, 2004; Ma et al., 2003; Matakatsu and Blair, 2004) (Fig. 8D,E). However, when Ds is overexpressed, Fat appears depleted from other membranes of

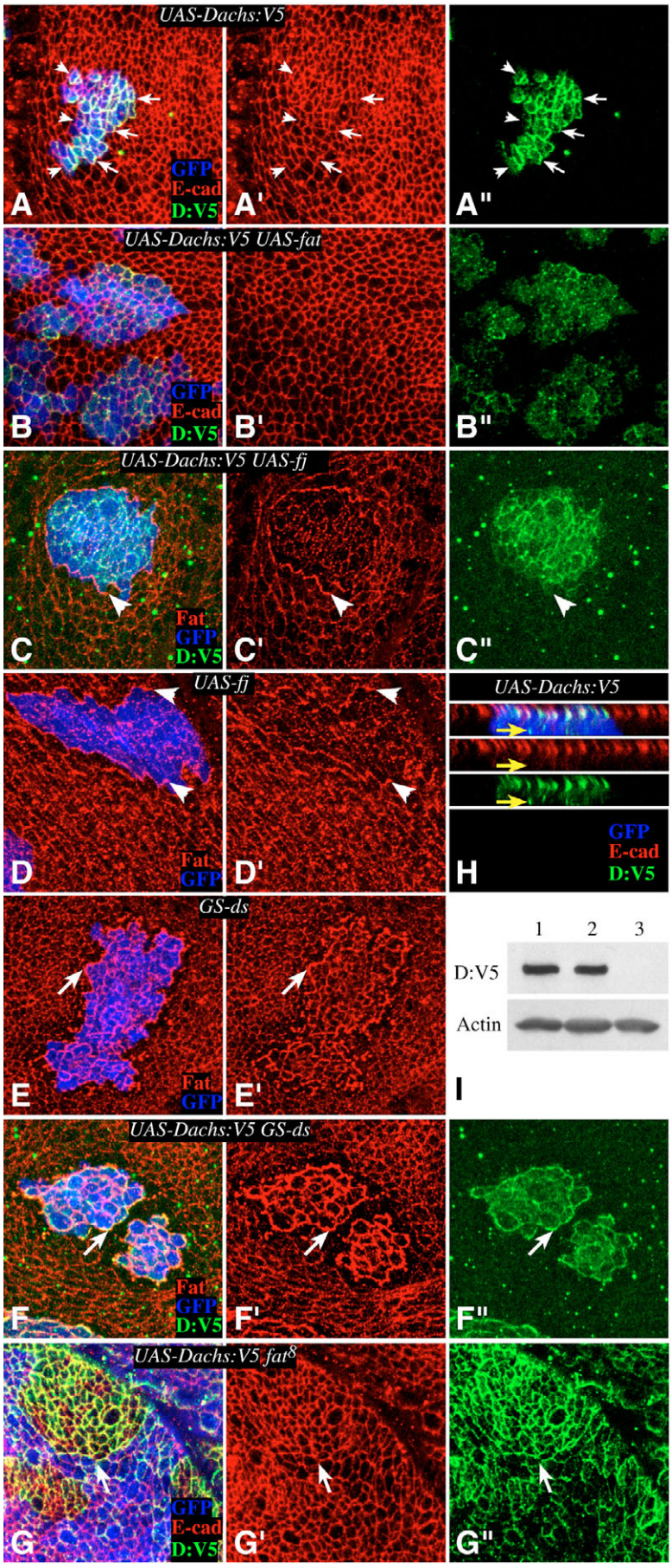

Fig. 8. Dachs protein localization. High magnifications of wing imaginal discs, stained for Fat (red, C-F) or E-cadherin (red, A,B,G) and Dachs:V5 (green), with GFP expression in blue. For experiments depicted in A and B, discs were treated in parallel, and images of clones were captured with identical confocal settings. (**A**) Dachs:V5-expressing clone in *AyGal4 UAS-dachs:V5[9F] UAS-GFP*. Arrows indicate distal clone edges with higher Dachs:V5; arrowheads indicate proximal clone edges with lower Dachs:V5. (**B**) Fat and Dachs:V5-expressing clone in *AyGal4 UAS-fat UAS-dachs:V5[9F] UAS-GFP*. (**C**) Fj and Dachs:V5-expressing clone in *AyGal4 UAS-dachs:V5[9F] UAS-fj[6a2] UAS-GFP*. Arrowhead indicates elevation of Fat, and coincident absence of Dachs:V5, at the edge of the clone. (**D**) Fj-expressing clone in *AyGal4UAS-fj[6a2] UAS-GFP*. Arrowhead indicates elevation of Fat at the edge of the clone. (**E**) Ds-expressing clone in *AyGal4 GS-ds UAS-GFP*. Arrow indicates elevation of Fat at the edge of the clone. (**F**) Ds and Dachs:V5-expressing clone in *AyGal4 UAS-dachs:V5[9F] GS-ds UAS-GFP*. Arrow indicates elevation of Fat, and coincident elevation of Dachs:V5, at the edge of the clone. (**G**) *fat* mutant clone (arrow), marked by absence of GFP, in *tub-Gal4 UAS-dachs:V5[18-2]*. Dachs staining is slightly elevated within the clone. (**H**) Vertical section through the apical-most 4.5 μm of the clone depicted in A. Most Dachs:V5 staining overlaps E-cadherin at the apical junctions, but there are discrete puncta (arrow), as well as more diffuse staining, in the cytoplasm. (**I**) Western blot, with anti-V5 or ant-Actin (control) on discs from: (1) $fat^{8}/fat^{G\text{-}rv}$; *tub-Gal4/UAS-dachs:V5[18-2]*, (2) $fat^{8}/+$; *tub-Gal4 /UAS-dachs:V5[18-2]* and (3) wild type.

neighboring cells (Fig. 8E,F), suggesting that the elevated Fat staining at the edge of Ds-expressing clones represents Fat protein in neighboring cells recruited to cellular interfaces where it can bind higher levels of Ds (Fig. 9D) (Cho and Irvine, 2004; Matakatsu and Blair, 2004). Conversely, when Four-jointed is overexpressed, Fat staining can appear partially depleted from other membranes of cells just inside the clone border (Fig. 8C,D). This suggests that the elevated Fat staining at the edge of Fj-expressing clones represents Fat protein recruited from cells inside the clone (Fig. 9C).

Because Dachs:V5 protein was expressed under UAS-Gal4 control, Dachs:V5 staining in these experiments was specifically detected within Ds- or Fj-expressing clones. Strikingly, these manipulations had opposite affects on Dachs. Overexpression of Ds was associated with elevated Dachs:V5 staining at the edges of the clone, while overexpression of Fj was associated with loss of Dachs:V5 staining at the edges of the clone (Fig. 8C,F). Given the Fat staining profile, these observations suggest that accumulation of Fat protein at the membrane inhibits the localization or stability of Dachs. This inference is consistent with the genetic epistasis of *dachs* to *fat*, and is further supported by the observation that removal of *fat* within clones of cells was associated with an increase in Dachs staining at the membrane (Fig. 8G), whereas overexpression of Fat was associated with a decrease in Dachs staining at the membrane (Fig. 8B). When Dachs:V5 levels in wild-type and *fat* mutant wing discs were compared by western blotting, there was no detectable difference (Fig. 8I). Thus, if Dachs stability is affected by Fat, Dachs at the membrane must represent only a small fraction of the total protein. As this does not appear to be the case (Fig. 8A,H), we suggest that the influence of Fat on Dachs protein staining most probably reflects protein re-localization.

Fj is expressed most strongly by distal wing cells, while Ds is expressed most strongly by proximal wing cells (Brodsky and Steller, 1996; Clark et al., 1995; Villano and Katz, 1995). Thus, if Fj and Ds normally influence Dachs protein localization, there might be some asymmetry in Dachs localization even in wild-type animals. Within the middle of clones expressing Dachs:V5, polarization of staining can not be assessed because the resolution of confocal microscopy can not distinguish which of two neighboring cells is contributing membrane staining. However, at the edges of Dachs:V5-expressing clones, all staining observed comes from a single cell. Importantly then, examination of clones of Dachs:V5-expressing cells in the wing pouch revealed that Dachs:V5 staining is generally stronger along the distal sides of the clones, and weaker along the proximal sides (Fig. 8A; 64/79 clones were scored as

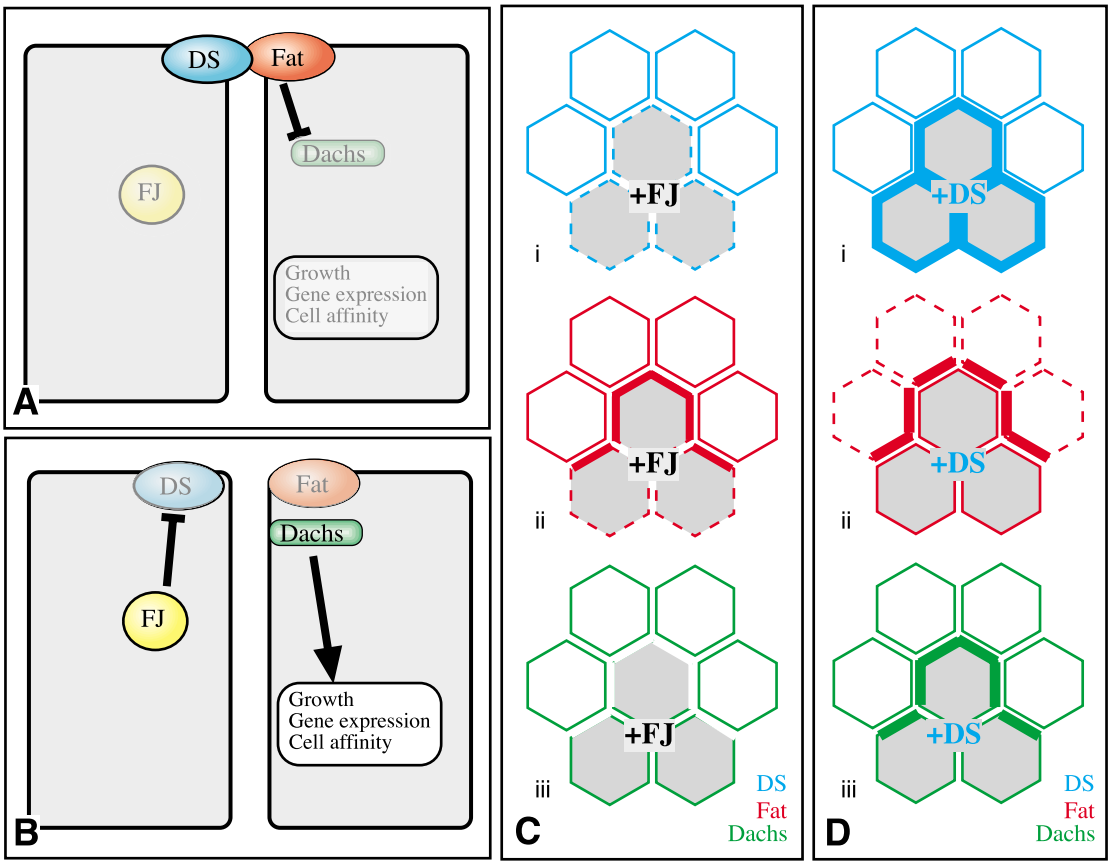

Fig. 9. Working models for Fat regulation and signaling. (A,B) Schematics of a cross-section of two cells. Genetic and protein localization studies position Dachs downstream of Fat in a pathway that influences growth and gene expression in imaginal discs. (**A**) When Ds and Fat are engaged, Fat accumulates at the membrane, where it downregulates Dachs, thereby preventing Dachs-dependent growth and gene expression. (**B**) Four-jointed is proposed to modify Ds and thereby prevent it from engaging Fat. This allows accumulation of Dachs, and promotion of growth, affinity and gene expression. (**C**,**D**) Show schematics of a horizontal section of a field of cells, with localization of Ds (blue), Fat (red) and Dachs (green) schematized. (C) Expression of Fj in a clone of cells (gray) is proposed to antagonize Ds (i) (broken lines). The absence of a good Ds partner within the clone causes Fat in cells at the edge of the clone to localize to the clone perimeter (ii), where it downregulates Dachs (iii). (D) Expression of Ds in a clone of cells (i) (gray) is proposed to recruit Fat in neighboring cells to the edge of the clone (ii). This results in elevated Dachs at the edge of the clone (iii). See text for discussion of possible mechanisms.

having elevated Dachs on the distal side, 15/79 were scored as having no significant difference, and 0/79 were scored as having stronger Dachs:V5 on the proximal side). This observation implies that asymmetric localization of Dachs in response to regulation of Fat occurs during normal development, and at endogenous expression levels of Fj and Ds.

DISCUSSION

Dachs is a downstream component of a Fat signaling pathway

The observation that a hypomorphic mutation of *dachs* could suppress the effects of *fat* mutations on wing growth and Wg expression in the proximal wing led to the suggestion that *dachs* might act as a downstream component of a Fat signaling pathway (Cho and Irvine, 2004). Here, we have provided two types of evidence that confirm this suggestion. First, *dachs* is epistatic to *fat* for multiple phenotypes in multiple tissues, including gene expression, growth and cell affinity. Indeed, with the notable exception of the influence of *fat* on tissue polarity, all known *fat* mutant phenotypes are completely suppressed by mutation of *dachs*. Second, we found that expression of regulators of Fat, Fj and Ds, or of Fat itself, influence the localization or stability of Dachs protein at the membrane, thus providing a molecular link from Fat to Dachs.

A myosin in the Fat pathway

The predicted structure of Dachs is unique within the myosin superfamily, and places Dachs in a new class of unconventional myosins. It has most similarity to myosins V, VII, and X. This is intriguing, as a mammalian protocadherin, Cdh23, has been functionally linked to myosin VIIa during the development of sensory hair cells in the inner ear (Boeda et al., 2002).

Within the myosin head region, the major conserved domains are all present, suggesting that Dachs functions as a motor protein. However, it is also possible that Dachs serves a structural or scaffolding role. For example, in the Hedgehog pathway, a kinesin-related protein, Costal2, is thought to function largely as a scaffold that brings together crucial kinases with their substrates (reviewed by Ogden et al., 2004).

The d^{GC2} mutation deletes part of the N terminal extension. As d^{GC2} mutants have relatively weak phenotypes, the N terminal extension might not be not essential for Dachs activity. Conversely, the severe phenotypes of alleles that truncate Dachs in the myosin head region imply that the myosin domain is essential. d^{GC13} in particular is predicted to eliminate almost all of the myosin head domain, and genetically it appears to act as a null allele.

Normal requirements for *dachs* in wing and leg growth

Characterization of new *dachs* alleles has provided an opportunity to define more clearly the requirements for *dachs*. *dachs* is required for normal wing and leg growth, although some appendage growth is *dachs* independent. Importantly, the identification of *dachs* as a downstream component of a Fat signaling pathway that influences growth implies that the reduced growth in *dachs* mutants is reflective of a normal role for a Fat pathway in growth promotion. That is, while *fat* is a gene whose normal role can be thought of as to restrain growth, as mutant tissue overgrows, we suggest that inhibition of Fat occurs during normal development, and that this inhibition contributes to normal appendage growth, as defined by the reduced growth of *dachs* mutants. Normal inhibition of Fat activity would presumably be effected by the two known regulators of Fat, Fj and Ds.

Whether available *dachs* mutations fully define the normal involvement of the Fat pathway in growth promotion is not yet clear. We cannot exclude the possibility that *dachs* is partially redundant with other proteins (e.g. other myosins), although this seems unlikely given the complete suppression of all non-polarity phenotypes of *fat* by *dachs*. It is also possible that *dachs* is required only for peak Fat signaling. This explanation is suggested by the observation that expression of the Fat target genes *wg*, *Ser* and *fj* is only partially or transiently lost in *dachs* mutants, yet the elevated or ectopic expression of these genes in *fat* mutants is completely eliminated by mutation of *dachs*.

Dachs and tissue polarity

The relatively mild tissue polarity phenotypes of *dachs* mutants, and the inability of *dachs* mutation to completely suppress the influence of *fat* on tissue polarity, contrast with the absolute dependence of *fat* gene expression, growth and affinity phenotypes on *dachs*. These observations suggest that there are two distinct Fat pathways. One, crucially dependent on Dachs, influences gene expression, growth and cell affinity, and another, partially independent of Dachs, influences tissue polarity. Studies of the atrophin protein Grunge also support the suggestion that there is a distinct Fat polarity pathway, as Grunge interacts with Fat and influences tissue polarity (Fanto et al., 2003), but does not exhibit other phenotypes observed in *fat* mutants (Cho and Irvine, 2004; Fanto et al., 2003). Thus, Dachs might act redundantly with another protein in a polarity pathway, but non-redundantly in a pathway that influences gene expression. It should also be noted that effects of *dachs* on gene expression might contribute to the polarity phenotypes of *dachs* mutants. For example, *fj* is regulated by *dachs* (Fig. 4), and *fj* has polarity phenotypes (Casal et al., 2002; Zeidler et al., 1999; Zeidler et al., 2000).

The asymmetric localization of Dachs observed in wild-type wings, and the influence of Fj and Ds on Dachs localization, have important implications for tissue polarity. First, the asymmetric localization of Dachs is itself a form of polarity, and its detection in third instar imaginal discs emphasizes that these cells are polarized well before core polarity proteins such as Frizzled and Dishevelled become asymmetrically localization in pupal wings (reviewed by Eaton, 2003). A similar conclusion can be drawn from the recent observation that *fat* and *ds* influence the orientation of cell divisions in third instar discs (Baena-Lopez et al., 2005). Second, our observations identify an ability to induce asymmetric protein localization as a mechanism through which the Fat pathway might influence tissue polarity. Dachs is one target, but the Fat polarity pathway might similarly involve asymmetric localization of other myosins, or of other types of proteins, to affect tissue polarity.

How does Fat signaling affect Dachs?

Mutation of *fat* is associated with elevated Dachs staining at the membrane, and overexpression of Fat decreases Dachs staining at the membrane. Although this negative effect of Fat on Dachs is subject to the caveat that we can only detect tagged overexpressed Dachs:V5, this tagged protein rescues *dachs* mutants, and the effects of Fat on Dachs staining are consistent with their opposite phenotypes and the epistasis of *dachs* to *fat*. Manipulations of the expression of Fat regulators provide further evidence that Fat regulates Dachs levels at the membrane, and altogether our observations implicate Dachs as a crucial intracellular component of a Fat signaling pathway (Fig. 9A,B).

The concomitant elevation of Fat staining and loss of Dachs staining observed at the perimeter of Fj-expressing clones is consistent with the conclusion that Fat can antagonize the

localization or stability of Dachs at the membrane. Because the elevation of Fat is limited to the periphery of Fj-expressing clones, we hypothesize that it results from an influence of Fj on Fat-Ds interactions, rather than the expression of Fj per se. Tissue polarity studies have implied that Fj and Ds have opposite affects on Fat. Although it has not yet been determined whether Fj can directly modify Fat or Ds, the simplest explanation for the elevated Fat staining at the edge of Fj-expressing cells would be to propose that Fj modifies Ds to inhibit its interactions with Fat (Fig. 9B). In this case, Fat protein within Fj-expressing clones would be predicted to prefer to bind to Ds outside of the clone, and hence to accumulate at the clone perimeter, where it would then downregulate Dachs (Fig. 9C).

The interpretation of the elevated Dachs staining at the perimeter of Ds-expressing clones is more complex. Although Fat is elevated at the clone perimeter, the depletion of Fat from neighboring cells suggests that the elevated Fat staining largely reflects Fat outside of the clone, rather than in Ds-expressing cells (Fig. 8E,F; Fig. 9D). Given that *dachs* and *fat* influence transcriptional targets cell autonomously, and *dachs* acts genetically downstream of *fat*, the link between elevated Fat in one cell and elevated Dachs in a neighboring cells must be indirect. It might be that Ds can also influence Dachs localization, and does so in opposite fashion to Fat. According to this scenario, the elevated Fat staining in cells neighboring the clone would be reflective of high levels of Ds engaged by Fat at the clone perimeter, which would then recruit or stabilize Dachs at the membrane. However, mutation of *ds* did not result in any noticeable decrease of Dachs:V5 staining (data not shown). Alternatively, it might be that Fat antagonizes the accumulation of Ds within the same cell. High Fat accumulation at the edge of one cell could then result in low Fat accumulation at the edge of its neighbor through this hypothesized downregulation of Ds. In this case, the elevated Dachs accumulation at the edge of Ds-expressing clones would be a consequence of low levels of Fat. This model would also imply that asymmetric localization of Fat could be propagated from cell to cell, which could have important consequences for Fat pathway regulation. However, there is as yet no evidence that Fat is asymmetrically localized at wild-type levels of Fj and Ds expression.

We thank F. M. Hoffmann, T. Schupbach, H. McNeill, M. Simon, S. Blair, the Developmental Studies Hybridoma Bank and the Bloomington stock center for antibodies and *Drosophila* stocks. We are especially grateful to F. Michael Hoffmann for providing us with unpublished mutant alleles. We thank Gerri Buckles and Olga Dunaevsky for excellent technical assistance. This work was supported by NSF grant IBN 9724930 (F.N.K.), NIH grant GM63057 (C.R.) and by the Howard Hughes Medical Institute (K.D.I.).

Supplementary material

Supplementary material for this article is available at http://dev.biologists.org/cgi/content/full/133/13/2539/DC1

References

Adler, P. N., Charlton, J. and Liu, J. (1998). Mutations in the cadherin superfamily member gene dachsous cause a tissue polarity phenotype by altering frizzled signaling. *Development* **125**, 959-968.

Baena-Lopez, L. A., Baonza, A. and Garcia-Bellido, A. (2005). The orientation of cell divisions determines the shape of Drosophila organs. *Curr. Biol.* **15**, 1640-1644.

Bingham, P. M. and Chapman, C. H. (1986). Evidence that white-blood is a novel type of temperature-sensitive mutation resulting from temperature-dependent effects of a transposon insertion on formation of white transcripts. *EMBO J.* **5**, 3343-3351.

Boeda, B., El-Amraoui, A., Bahloul, A., Goodyear, R., Daviet, L., Blanchard, S., Perfettini, I., Fath, K. R., Shorte, S., Reiners, J. et al. (2002). Myosin VIIa, harmonin and cadherin 23, three Usher I gene products that cooperate to shape the sensory hair cell bundle. *EMBO J.* **21**, 6689-6699.

Bridges, C. B. and Morgan, T. H. (1919). Contributions to the genetics of Drosophila melanogaster. II. The second-chromosome group of mutant characters. *Carnegie Inst. Washington Publ*. **278**, 123-304.

Brodsky, M. H. and Steller, H. (1996). Positional information along the dorsal-ventral axis of the Drosophila eye: graded expression of the four-jointed gene. *Dev. Biol.* **173**, 428-446.

Brown, N. H. and Kafatos, F. C. (1988). Functional cDNA libraries from Drosophila embryos. *J. Mol. Biol.* **203**, 425-437.

Bryant, P. J., Huettner, B., Held, L. I., Jr, Ryerse, J. and Szidonya, J. (1988). Mutations at the fat locus interfere with cell proliferation control and epithelial morphogenesis in Drosophila. *Dev. Biol.* **129**, 541-554.

Buckles, G. R., Rauskolb, C., Villano, J. L. and Katz, F. N. (2001). four-jointed interacts with dachs, abelson and enabled and feeds back onto the Notch pathway to affect growth and segmentation in the Drosophila leg. *Development* **128**, 3533-3542.

Casal, J., Struhl, G. and Lawrence, P. (2002). Developmental compartments and planar polarity in Drosophila. *Curr. Biol.* **12**, 1189-1198.

Chen, B., Chu, T., Harms, E., Gergen, J. P. and Strickland, S. (1998). Mapping of Drosophila mutations using site-specific male recombination. *Genetics* **149**, 157-163.

Cho, E. and Irvine, K. D. (2004). Action of fat, four-jointed, dachsous and dachs in distal-to-proximal wing signaling. *Development* **131**, 4489-4500.

Clark, H. F., Brentrup, D., Schneitz, K., Bieber, A., Goodman, C. and Noll, M. (1995). Dachsous encodes a member of the cadherin superfamily that controls imaginal disc morphogenesis in Drosophila. *Genes Dev.* **9**, 1530-1542.

Drysdale, R. A. and Crosby, M. A. (2005). FlyBase: genes and gene models. *Nucleic Acids Res.* **33**, D390-D395.

Duncan, D. M., Burgess, E. A. and Duncan, I. (1998). Control of distal antennal identity and tarsal development in Drosophila by spineless-aristapedia, a homolog of the mammalian dioxin receptor. *Genes Dev.* **12**, 1290-1303.

Eaton, S. (2003). Cell biology of planar polarity transmission in the Drosophila wing. *Mech. Dev.* **120**, 1257-1264.

FlyBase Consortium (1999). The FlyBase database of the Drosophila genome projects and community literature. *Nucleic Acids Res.* **27**, 85-88.

Fanto, M., Clayton, L., Meredith, J., Hardiman, K., Charroux, B., Kerridge, S. and McNeill, H. (2003). The tumor-suppressor and cell adhesion molecule Fat controls planar polarity via physical interactions with Atrophin, a transcriptional co-repressor. *Development* **130**, 763-774.

Hao, I., Green, R. B., Dunaevsky, O., Lengyel, J. A. and Rauskolb, C. (2003). The odd-skipped family of zinc finger genes promotes Drosophila leg segmentation. *Dev. Biol.* **263**, 282-295.

Held, L. I., Duarte, C. M. and Derakshanian, K. (1986). Extra tarsal joints and abnormal cuticular polarities in various mutants of Drosophila melanogaster. *Roux Arch. Dev. Biol.* **195**, 145-157.

Irvine, K. D. and Rauskolb, C. (2001). Boundaries in development: formation and function. *Annu. Rev. Cell Dev. Biol.* **17**, 189-214.

Kiehart, D. P., Franke, J. D., Chee, M. K., Montague, R. A., Chen, T. L., Roote, J. and Ashburner, M. (2004). Drosophila crinkled, mutations of which disrupt morphogenesis and cause lethality, encodes fly myosin VIIA. *Genetics* **168**, 1337-1352.

Klein, T. (2001). Wing disc development in the fly: the early stages. *Curr. Opin. Genet. Dev.* **11**, 470-475.

Korn, E. D. (2000). Coevolution of head, neck, and tail domains of myosin heavy chains. *Proc. Natl. Acad. Sci. USA* **97**, 12559-12564.

Lawrence, P. A. and Struhl, G. (1996). Morphogens, compartments, and pattern: lessons from drosophila? *Cell* **85**, 951-961.

Ma, D., Yang, C. H., McNeill, H., Simon, M. A. and Axelrod, J. D. (2003). Fidelity in planar cell polarity signalling. *Nature* **421**, 543-547.

Mahoney, P. A., Weber, U., Onofrechuk, P., Biessmann, H., Bryant, P. J. and Goodman, C. S. (1991). The fat tumor suppressor gene in Drosophila encodes a novel member of the cadherin gene superfamily. *Cell* **67**, 853-868.

Matakatsu, H. and Blair, S. S. (2004). Interactions between Fat and Dachsous and the regulation of planar cell polarity in the Drosophila wing. *Development* **131**, 3785-3794.

McLean, I. W. and Nakane, P. K. (1974). Periodate-tysine-paraformaldehyde fixative. A new fixation for immunoelectron microscopy. *J. Histochem. Cytochem.* **22**, 1077-1083.

Ogden, S. K., Ascano, M., Jr, Stegman, M. A. and Robbins, D. J. (2004). Regulation of Hedgehog signaling: a complex story. *Biochem. Pharmacol.* **67**, 805-814.

Papayannopoulos, V., Tomlinson, A., Panin, V. M., Rauskolb, C. and Irvine, K. D. (1998). Dorsal-ventral signaling in the Drosophila eye. *Science* **281**, 2031-2034.

Rauskolb, C. (2001). The establishment of segmentation in the Drosophila leg. *Development* **128**, 4511-4521.

Rauskolb, C. and Irvine, K. D. (1999). Notch-mediated segmentation and growth control of the Drosophila leg. *Dev. Biol.* **210**, 339-350.

Rawls, A. S., Guinto, J. B. and Wolff, T. (2002). The cadherins fat and dachsous regulate dorsal/ventral signaling in the Drosophila eye. *Curr. Biol.* **12**, 1021-1026.

Robertson, H. M., Preston, C. R., Phillis, R. W., Johnson-Schlitz, D. M., Benz,

W. K. and Engels, W. R. (1988). A stable genomic source of P element transposase in Drosophila melanogaster. *Genetics* **118**, 461-470.
Strutt, H. and Strutt, D. (2002). Nonautonomous planar polarity patterning in Drosophila: dishevelled-independent functions of frizzled. *Dev. Cell* **3**, 851-863.
Strutt, H., Mundy, J., Hofstra, K. and Strutt, D. (2004). Cleavage and secretion is not required for Four-jointed function in Drosophila patterning. *Development* **131**, 881-890.
Tzolovsky, G., Millo, H., Pathirana, S., Wood, T. and Bownes, M. (2002). Identification and phylogenetic analysis of Drosophila melanogaster myosins. *Mol. Biol. Evol.* **19**, 1041-1052.
Villano, J. L. and Katz, F. N. (1995). four-jointed is required for intermediate growth in the proximal-distal axis in Drosophila. *Development* **121**, 2767-2777.
Waddington, C. H. (1940). The genetic control of wing development in Drosophila. *J. Genet.* **41**, 75-139.
Waddington, C. H. (1943). The development of some 'leg genes' in Drosophila. *Drosophila. J. Genet.* **45**, 29-43.
Yang, C., Axelrod, J. D. and Simon, M. A. (2002). Regulation of frizzled by fat-like cadherins during planar polarity signaling in the Drosophila compound eye. *Cell* **108**, 675-688.
Zeidler, M. P., Perrimon, N. and Strutt, D. I. (1999). The four-jointed gene is required in the Drosophila eye for ommatidial polarity specification. *Curr. Biol.* **9**, 1363-1372.
Zeidler, M. P., Perrimon, N. and Strutt, D. I. (2000). Multiple roles for four-jointed in planar polarity and limb patterning. *Dev. Biol.* **228**, 181-196.